Early Detection of Heterotopic Ossification Using Near-Infrared Optical Imaging Reveals Dynamic Turnover and Progression of Mineralization Following Achilles Tenotomy and Burn Injury

Joseph E. Perosky,[1] Jonathan R. Peterson,[2] Owulatobi N. Eboda,[2] Michael D. Morris,[3] Stewart C. Wang,[2] Benjamin Levi,[2] Kenneth M. Kozloff[1]

[1]Department of Orthopaedic Surgery, University of Michigan, [2]Department of Plastic Surgery, University of Michigan, [3]Department of Chemistry, University of Michigan

Received 5 May 2014; accepted 24 June 2014
Published online 2 August 2014 in Wiley Online Library (wileyonlinelibrary.com). DOI 10.1002/jor.22697

ABSTRACT: Heterotopic ossification (HO) is the abnormal formation of bone in soft tissue. Current diagnostics have low sensitivity or specificity to incremental progression of mineralization, especially at early time points. Without accurate and reliable early diagnosis and intervention, HO progression often results in incapacitating conditions of limited range of motion, nerve entrapment, and pain. We hypothesized that non-invasive near-infrared (NIR) optical imaging can detect HO at early time points and monitor heterotopic bone turnover longitudinally. C57BL6 mice received an Achilles tenotomy on their left hind limb in combination with a dorsal burn or sham procedure. A calcium-chelating tetracycline derivative (IRDye 680RD BoneTag) was injected bi-weekly and imaged via NIR to measure accumulative fluorescence for 11 wk and compared to in vivo microCT images. Percent retention of fluorescence was calculated longitudinally to assess temporal bone resorption. NIR detected HO as early as five days and revealed a temporal response in HO formation and turnover. MicroCT could not detect HO until 5 wk. Confocal microscopy confirmed fluorophore localization to areas of HO. These findings demonstrate the ability of a near-infrared optical imaging strategy to accurately and reliably detect and monitor HO in a murine model. © 2014 Orthopaedic Research Society. Published by Wiley Periodicals, Inc. J Orthop Res 32:1416–1423, 2014.

Keywords: heterotopic Ossification; molecular imaging; microCT; biomarkers

Heterotopic ossification (HO) is a debilitating condition resulting in abnormal formation of bone in soft tissue. Common causes include trauma, burns, orthopaedic surgery, traumatic brain injury, or a combination of these events.[1,2] Without accurate and reliable early diagnosis and intervention, progression often results in joint contractures, nerve entrapment, and pain.[1,2] Resolution of HO requires invasive surgery, leaving >75% of patients with functional deficits.[2]

Early intervention combined with common prophylactic treatments such as NSAIDs or single dose radiation therapy[3–6] protects against recurrence of HO formation, in addition to an easier surgery, quicker, more effective rehabilitation, and improved viability of surrounding tissue.[7,8] Therefore, the development of a sensitive diagnostic modality that can detect HO at early time points would greatly improve clinical care of HO patients.

Radiographic techniques, including computed tomography (CT) and magnetic resonance imaging (MRI), provide high resolution visualization of late stage HO; however, they have low sensitivity to incremental progression of mineralization and difficulty differentiating HO from surrounding soft tissue, especially early.[9–12] Combined MRI and CT aids in the early diagnosis of HO; however, this relies on a "wait and see" approach to monitor changes in mineralization over time, which may be unsuitable for diagnosing cases where progression can be detrimental.[13] CT and MRI can also be time-consuming and expensive, particularly in longitudinal imaging.

Three-phase bone scintigraphy (SPECT) is used for early HO detection.[2] However, presence of inflammation or callus formation, which commonly accompany ectopic bone formation, may cause false positives during normal tissue healing when HO is not present and a high level of variability.[14,15] The absolute quantification of SPECT signals is complicated by factors including photon scatter and attenuation, necessitating complex corrective algorithms.[16] Ultrasound can detect HO sooner than conventional radiography, but cannot distinguish new bone formation from less mineralized mature bone.[17,18]

Therefore, the capability to accurately diagnose HO formation and progression would ensure the greatest benefit of treatment therapies and minimize complications from unnecessary prophylaxis. Non-invasive near-infrared (NIR) fluorescence imaging modalities have the potential to diagnose bone mineralization and bone turnover at multiple time points.[19] NIR can achieve high tissue penetration of light and low tissue autofluorescence within the NIR spectrum[20] and allows for the visualization of multiple contrast agents at nanomolar levels.[21] NIR imaging techniques have been used to monitor exogenous contrast agents associated with bone mineralization, resorption, and skeletal drug delivery in rodent models of development, repair, and disease,[19,22,23] and advanced techniques are currently being investigated for humans.[24]

HO is believed to be formed primarily in the context of endochondral ossification. Currently, animal models exist for studying HO, but many rely on implantation of osteogenic cells or media implanted in the soft

Grant sponsor: NIH; Grant numbers: R01 AR056646, K08 GM109105; Grant Sponsor: Plastic Surgery Foundation National Endowment Award.
Correspondence to: Kenneth M. Kozloff (T: +734-936-2158; F: +734-647-0003; E-mail: kenkoz@umich.edu)

tissue, which is not analogous to the clinical scenario. Therefore, a mouse model that is similar to the causation of clinical HO was utilized. This model involves local tendon damage and systemic inflammation caused by a burn, which are both common causes of HO, and results in spontaneous HO formation. [1,25] We evaluated the ability of NIR imaging to noninvasively monitor the progression of HO in vivo in a mouse model.

METHODS

Experimental Design

Seven to eight week old male C57BL6 mice underwent a unilateral Achilles tenotomy with or without an accompanying dorsal partial thickness burn injury ($N = 7$/group). The burn injury consisted of immersion of 30% of the mouse dorsum in a water bath for 18 s (sham = 30°C, burn = 60°C). This procedure accelerates HO formation at the tenotomy site.[26] HO was then measured longitudinally using NIR optical imaging and microCT for 11 wk. Findings were confirmed via endpoint histology. All studies were approved by the University of Michigan Committee on Use and Care of Animals.

Assessment of Probe Specificity and Distribution

To assess the optimal timing for fluorescent imaging probe delivery, longitudinal imaging was performed on three 10 wk-old female Balb/C mice injected with a cocktail of IRDye 680RD BoneTag (160 nmoles/kg; LI-COR Biosciences, Lincoln NE) and IRDye 800 CW Carboxylate (80 nmoles/kg; LI-COR Biosciences). The former probe is an NIR calcium-chelating tetracyline derivative with maximum wavelengths of 675 nm absorption and 697 emission. [27] The latter probe is a spectrally distinct (774 nm absorption/788 nm emission), non-reactive control dye used to assess non-specific clearance through the bloodstream and tissues. Mice were imaged as described below at baseline, prior to injection, and subsequently at 5 min and 2, 6, 12, 24, 48, and 72 h to assess BoneTag binding versus non-specific vascular perfusion at the proximal tibia.

In Vivo Near-Infrared Optical Imaging of Heterotopic Ossification

At 5 days, and every 2 wk following for 11 wk, mice received 80 nmole/kg of IRDye 680RD BoneTag (LI-COR Biosciences) in 100 μL PBS via tail-vein injection while anesthetized. This contrast agent is an NIR calcium-chelating tetracycline derivative, with maximum wavelengths of 675 nm absorption and 697 nm emission.[27] Prior to each injection, mice were imaged using a multi-spectral acquisition system (Pearl Impulse, LI-COR Biosciences, 685 nm excitation) to quantify baseline levels of tissue fluorescence. Mice were subsequently imaged 24 hrs post-injection to quantify the amount of newly-bound BoneTag fluorophore at each time point.

HO was assessed by measuring total fluorescence of BoneTag in regions of interest of the posterior calcaneus and mid-tibia. Regions of interest were identified on brightfield images and then overlaid on fluorescence images to quantify the total fluorescence for each specimen, as a sum of the fluorescence in the posterior calcaneus and mid-tibia. The amount of fluorescence present before injection was subtracted from the amount measured 24 hrs after injection to quantify the amount of probe delivered for each 2 wk time period. The Accumulative Fluorescence through the duration of the study was calculated by summing the fluorescence at each time point and used as a surrogate marker for how much total heterotopic bone was formed (Equation 1). To assess temporal resorptive activity, Percent Retention of the BoneTag fluorophore during each 2 wk period was calculated by subtracting the amount of retained fluorophore measured in the pre-injection image from the post-injection image of the previous time point (Equation 2).

$$\begin{aligned}\text{Accumulative Fluorescence}_N &= (\text{Postinjection} - \text{Preinjection})_1 \\ &+ (\text{Postinjection} - \text{Preinjection})_2 \\ &+ \cdots + (\text{Postinjection} - \text{Preinjection})_N\end{aligned} \quad (1)$$

$$\text{Percent Retention}_{N \text{ to } N+1} = \text{Postinjection}_N - \text{Preinjection}_{N+1} \quad (2)$$

In Vivo MicroCT

While still anesthetized, mice were imaged using microCT (GE Healthcare Pre-Clinical Imaging, London, Ontario). Images were reconstructed at an isotropic voxel size of 45 μm and calibrated for densitometry. Regions of interest analogous to those used for NIR focused on the distal calcaneus and mid-tibia and were isolated and assessed (MicroView v2.2, GE Healthcare Pre-Clinical Imaging) to measure HO volume independent of pre-existing native bone. A global threshold of 1000 Hounsfield Units was applied for assessment.

Ex Vivo Near-Infrared Optical Imaging

At 11 wk, mice were euthanized, and tibiae and calcanei were removed together, minimally dissected, and imaged by NIR (Pearl Impulse, LI-COR Biosciences). Regions of interests akin to those used to assess the in vivo NIR images were used to measure HO ex vivo.

Ex Vivo MicroCT

Tibia and calcanei were then analyzed by microCT (eXplore Locus SP, GE Healthcare Pre-Clinical Imaging). Specimens were immersed in water and scanned two at a time using the Parker method (180° plus a 20° fan angle) of rotation at 80 kVp and 80 μA with added filtration in the form of both an acrylic beam flattener and a 0.02 inch aluminum filter. Images were reconstructed at 18 μm voxel size and calibrated for densitometry.

Histology

To examine probe localization within the HO sites, tibiae and calcanei were fixed in 10% NBF for 24 hrs, dehydrated in 70% EtOH, processed, and embedded in PMMA as previously described.[28] Thick sections were cut (EXAKT 300 CP, EXAKT Technologies, Inc. Norerstedt, Germany) and polished to a thickness of ~250 μm (EXAKT 400 Micro Grinding System, EXAKT Technologies). Images of probe localization in HO and in normal cortical and trabecular bone were taken using confocal microscopy (Leica Upright SP5X Confocal Microscope, Leica Microsystems, Wetzlar, Germany) with 10x objectives. Images from 3 consecutive sections were taken to confirm consistency. The same sections were then stained with toluidine blue to confirm tissue general tissue features.[29]

Data Analysis

HO progression and probe resorption over the 11 wk time course measured by accumulative fluorescence and percent of fluorophore retention and bone volume measured by microCT were assessed by mixed model and within-sample repeated measures ANOVA followed by Bonferroni post-hoc tests. A linear regression was conducted to determine ability of microCT bone volume to predict in-vivo NIR fluorescence accumulation. Data are presented as mean ± std dev. All data were analyzed using IBM SPSS Statistics V.21 (SPSS, Inc., Chicago, IL. Significance was represented as $p < 0.05$ unless stated otherwise.

RESULTS

Probe Distribution

Vascular perfusion of BoneTag680 and the carboxylated control probe was rapid, with significant proximal tibial signal within 5 min of injection (Fig. 1). IRDye 800CW signal subsequently declined between 5 min and 12 h, demonstrating rapid vascular clearance. In contrast, BoneTag signal peaked at 2 h, and then gradually declined to stable levels by 24 hrs post-injection, where signal remains ~70 times that of the carboxylated control (Fig. 1). These findings indicated 24 h as an optimal time for imaging post-injection.

In Vivo NIR Optical Imaging

In vivo NIR imaging revealed ectopic bone formation as early as 5 days in tenotomized limbs of burn and sham groups as compared to their contralateral controls, which progressed temporally at each time point (Fig. 2A,B). A significant difference in ossification between the 60° burn and 30° sham groups was observed at 5 wk, with a trend towards differences at 7, 9, and 11 wk ($p < 0.10$). Progression of HO was evident in the temporal NIR imaging sequence (Fig. 3), where both calcaneal and mid-soleus HO could be seen early on in the 60° group, and later in the 30° animals. Non-specific probe accumulation was evident in contralateral limbs of mice from both groups in the ankle, foot, and proximal tibial growth plates, with background levels well below those of operated limbs.

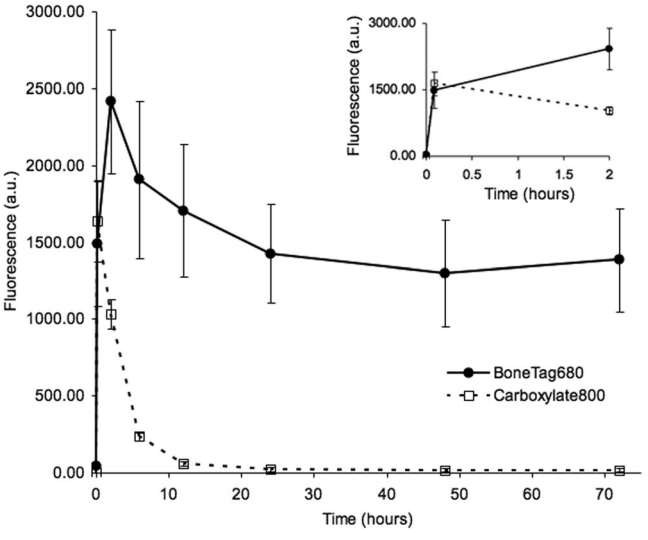

Figure 1. Time course of BoneTag distribution at the proximal tibia. Mice injected with BoneTag680 or a carboxylated control probe demonstrated early vascular perfusion of both imaging agents. BoneTag680 was retained specifically at skeletal sites, while the control probe was rapidly cleared through the vasculature after 5 min and virtually absent at 24 h. Inset: Probe fluorescence over initial 2 h magnified for clarity.

In addition to newly forming HO, local bone resorption was also temporal in nature. There was a decrease in fluorophore retention between 5 days and 3 wk compared to percent retention from 5 wk and beyond (Fig. 4A). This decrease retention is suggestive of an increase in resorptive activity between 5 days and 3 wk compared to 5 wk and beyond in the tenotomized limbs. Non-operated control limbs showed stable fluorophore retention, reflecting stability of turnover at non-HO sites (Fig. 4B).

In Vivo MicroCT

In vivo microCT was unable to detect HO until 5 wk, beyond which temporal progression of HO was consistent with that observed by in vivo NIR imaging (Fig. 2C). The response to the systemic inflammatory burn also produced an increase in HO bone volume at 5, 7, and 9 wk as compared to the tenotomy only group. Beyond 5 wk, microCT was predictive of accumulative fluorescence as a measurement of HO ($r^2 = 0.63$, $p < 0.0005$, Fig. 2D).

Ex Vivo Imaging and Histologic Assessment

High resolution ex vivo NIR optical imaging confirmed high probe accumulation at the posterior calcaneus and mid-soleus, consistent with ex vivo microCT scans (Fig. 5). Confocal microscopy revealed BoneTag probe within mature cortical bone and in areas of HO. Mid-tibial HO was woven and unorganized in nature (Fig. 6A-C) in contrast to the well-organized sequential labeling of the tibia (Fig. 6D, E). Toluidine blue staining confirmed mineralized bone tissue distinct from surrounding soft tissues.

Microscopic imaging of the bound BoneTag fluorophore to the HO posterior to the calcaneous was highly unorganized and trabecular in nature (Fig. 6F, H). Consistently across specimens, a "shell" of mature bone with trabecular-like woven bone inside was observed (Fig. 6F, G). These trabecular spicules were labeled with one or two distinct lines of BoneTag, reflecting the high turnover at this site. Conversely, fluorescence labeling of the posterior calcaneus was well organized and sequential in nature (Fig. 6J). Toluidine blue staining showed the distinction between mineralized bone tissue, surrounding soft tissues, and non-mineralized tissue within the HO regions of interest (Fig. 6G, I, K).

DISCUSSION

In a mouse model of HO, longitudinal NIR imaging revealed increased accumulative fluorescence in teno-

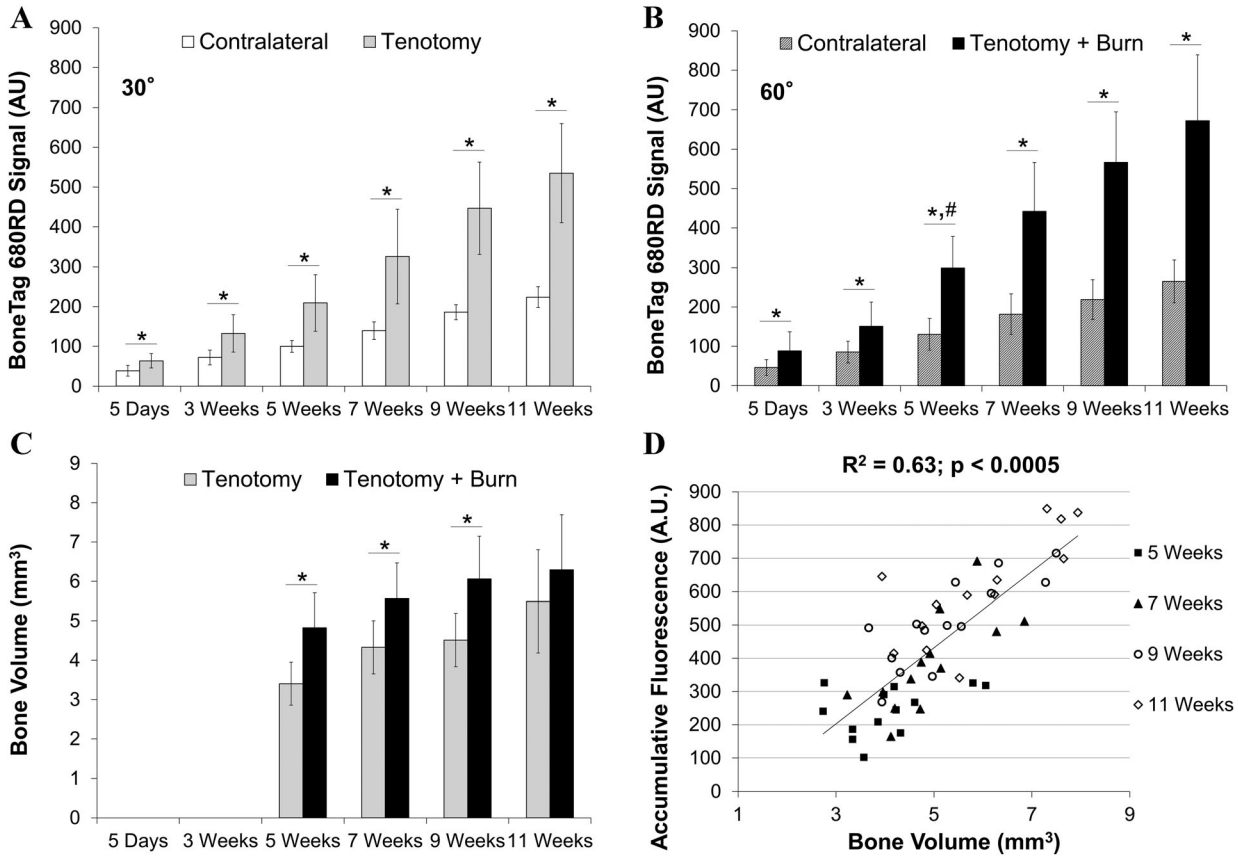

Figure 2. (A) Accumulative fluorescence in limbs subject to Achilles tenotomy was greater than contralateral controls in both (A) 30° and (B) 60° burn groups ($^{*}p < 0.05$ tenotomy vs. control). In both tenotomy groups, accumulative fluorescence significantly increased in a temporal manner. (B) Burn significantly accelerated HO by 5 wk over tenotomy alone (# $p < 0.05$ tenotomy + burn (B) versus tenotomy (A) with a trend toward continuing differences at 7, 9, and 11 wk ($p < 0.10$). (C) Heterotopic ossification was not detected by microCT until 5 wk. (D) Once detected, microCT was highly predictive of accumulative fluorescence; $R^2 = 0.63$, $p < 0.0005$.

tomized limbs at sites of extraskeletal bone formation compared to contralateral control limbs. Furthermore, NIR could differentiate the acceleration of HO in mice receiving an isolated dorsal burn at 5 wk post-injury. Interestingly, NIR could detect heterotopic mineralization earlier than microCT, which even at a resolution 20X greater than that used clinically[21] was unable to detect HO formation above mineralized thresholds

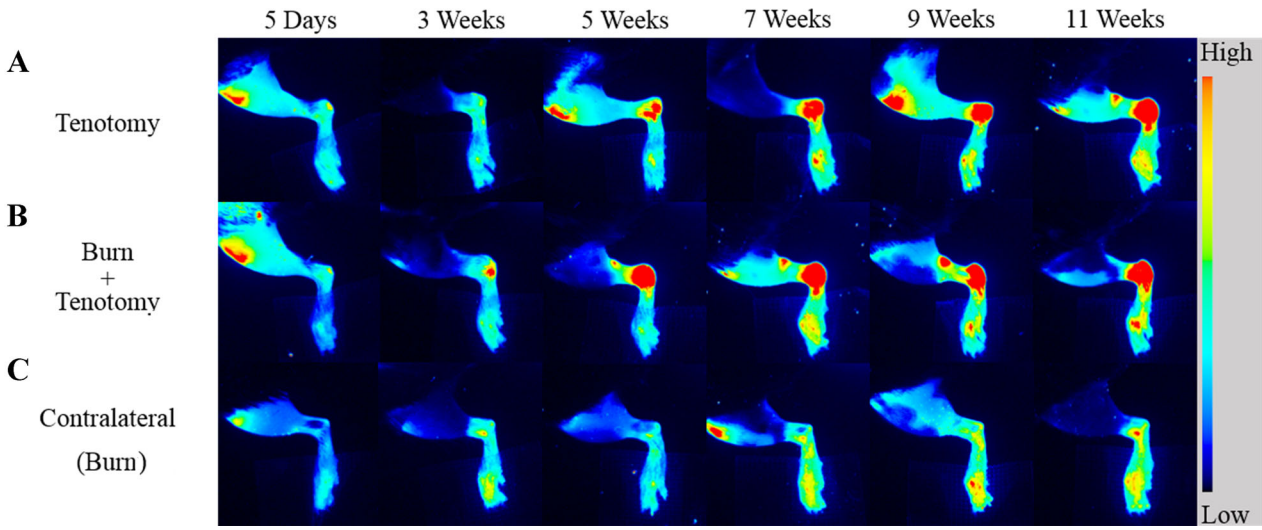

Figure 3. Temporal progression of heterotopic ossification was visualized by NIR imaging for (A) 30° tenotomy limbs and (B) tenotomy plus burn limbs. (C) Intact contralateral limbs from the burn group, which did not form HO are shown for comparison.

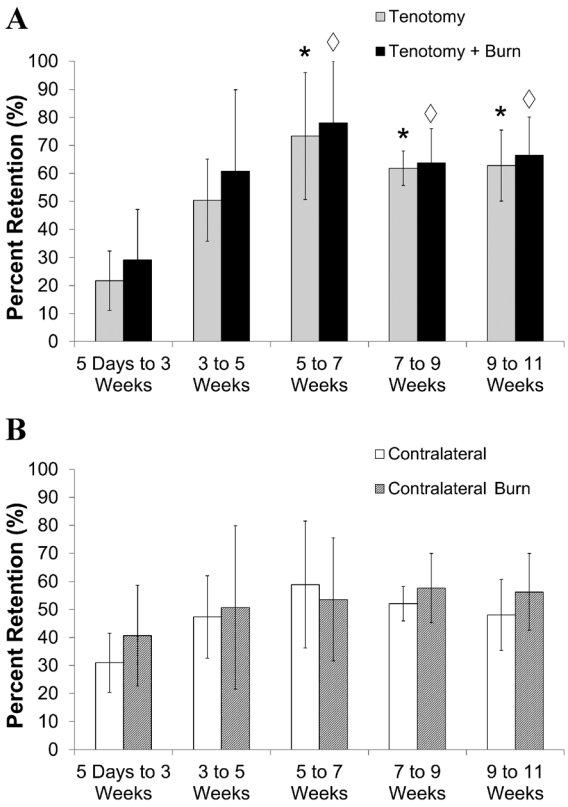

Figure 4. (A) Percent retention of fluorescence was significantly lower from 5 days to 3 wk compared to the 5–7, 7–9, and 9–11 wk time points (*, ◇ = $p < 0.05$ for tenotomized and tenotomized + burn groups respectively), indicating increased localized resorptive activity in both the tenotomy and tenotomy + burn groups until 3 wk, which normalizes by 5 wk. (B) This is in contrast to the contralateral limbs of both groups, which did not show any changes in fluorophore retention over time course.

until 5 wk in our model. This inability of radiography to detect HO at early time points is analogous to the clinical setting, where radiographic techniques are of limited utility in the early detection of HO formation. These detection limits could likely be improved with increased radiographic image resolution, but this may require greater associated radiation exposure and longer scan times, limiting the potential gains in image fidelity. Here, NIR could detect small amounts of early mineralization prior to our CT measures, consistent with our prior work using non-invasive Raman spectroscopy to detect early mineralization changes associated with HO in this same model.[26] Together, these findings suggest a benefit for optical technologies at assessing either chemical changes or focal mineralization through exogenous contrast agents associated with HO.

Fluorochrome-labeled biopsies have been used to monitor heterotopic ossification progression histology.[30] By using a tetracycline derivative with wavelengths shifted to the near-infrared, we have expanded the ability to detect HO to in vivo by imaging at wavelengths that have increased tissue penetration in the context of reduced background autofluorescence.[20] Confocal microscopy validated our in vivo observations. The NIR probe localized to areas of HO, but was also distributed throughout the existing ossified tissue. Labeling of HO revealed a woven and disorganized bone appearance, while neighboring mid-tibial and posterior calcaneal bone demonstrated a well-organized lamellar bone with multiple sequential labels, reflecting the continued growth of these animals over the entire 11 wk. This non-HO labeling was apparent

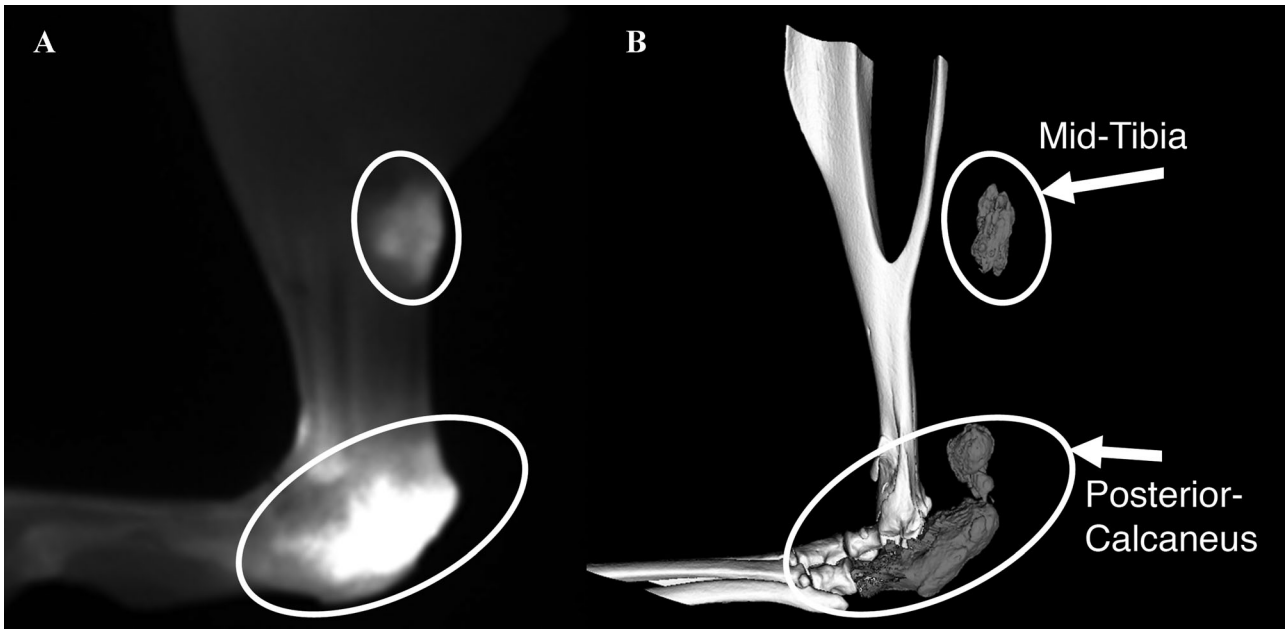

Figure 5. Ex vivo near-infrared (A) and microCT (B) images taken at 11 wk confirm the formation of mid-tibial HO, as well as HO formed around and on top of the posterior calcaneus. Formation of HO in the mid-tibia as well as the posterior-calcaneus was observed in all mice by cessation of observation at 11 wk time point.

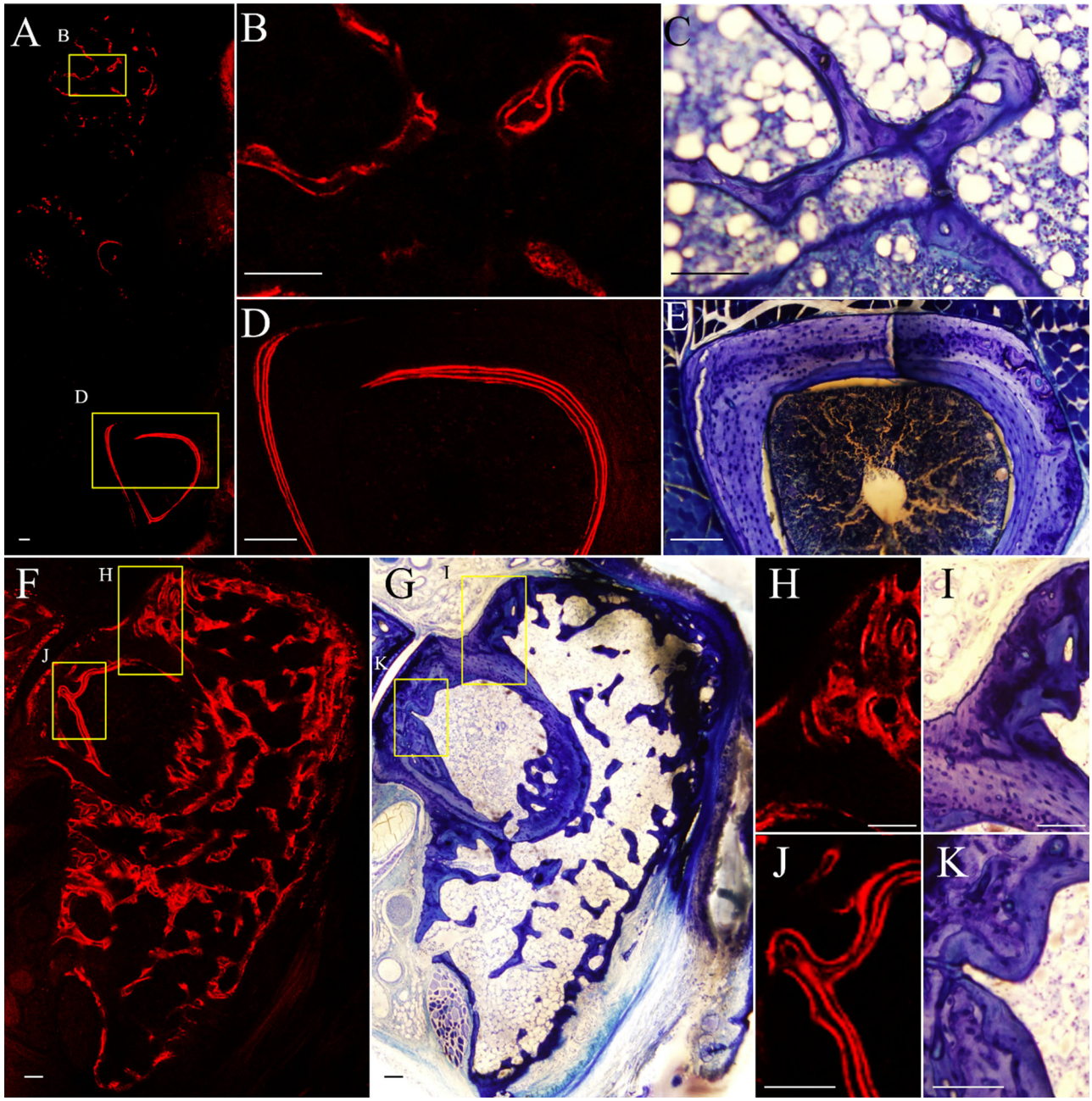

Figure 6. (A) confocal microscopy of mid-tibia region confirmed probe binding in regions of HO (B) as well as pre-existing cortical bone (D). Subsequent staining with toluidine blue confirmed HE (C) and cortical bone (E) phenotype. Confocal image of posterior calcaneous and corresponding (G) toluidine blue-stained section. (H,I): Unorganized HO formed on top of well-organized cortical bone (J,K). Scale bar = 100 μm.

in contralateral limbs, where fluorophore accumulated due to the animal growth, but remained less than tenotomy limbs as HO progressed.

Currently, the underlying molecular mechanisms responsible for HO are not well understood, but an increase in BMP levels is thought to cause mesenchymal stem cells to differentiate down osteogenic and chondrogenic lineages, thus stimulating endochondral ossification at non-bone sites, dependent on the native tissue. In addition to the progressive mineralization found at our HO sites, we observed dynamic turnover of HO at early time points. Previous work showed that HO results from increased inflammation in this model,[26,31] and in the present study we found HO to be accelerated when tenotomy was accompanied by burn at sites distant from the tenotomy injury. Few studies have looked at the resorptive activity associated with HO,[32] and due to the longitudinal nature of our study, we were unable to assess histology or endpoint imaging at early time points. Interestingly, the inflammato-

ry markers IL-6 and TNF-α, which are both elevated at early time points in HO,[31,33] were also shown to synergistically increase osteoclast differentiation and resorption.[34] The early loss of fluorescence in limbs subject to tenotomy, but not contralateral controls, may reflect an early turnover phenotype in this model that subsequently stabilizes as HO progresses. Further investigation into the physiological mechanisms underlying this dynamic turnover may provide insight into novel treatment therapies designed to interrupt this early remodeling process. Significantly, the early detection potential for this model allows for further investigations into both the formation and resorption mechanisms responsible for HO, which could lend insight into potential future therapy options.

Previous studies using this contrast agent demonstrated a linear increase in fluorescence signal with increasing doses in vivo and in vitro without signal saturation[27], suggesting ability to quantify HO, particularly at the low levels of mineralization when HO identification is most challenging. Translation to the clinic may require alternative visualization approaches, since traditional planar fluorescence imaging of NIR agents is restricted to several millimeters of tissue depth due to light penetration limitations and non-linear relationships between signal strength, depth of probe, and optical properties of the tissue.[35] Therefore, the use of handheld devices relying on planar illumination and imaging may be limited to sites nearest the skin surface, or during intraoperative procedures where NIR-guided imaging for resection of mineralization could be used in an open surgical site.[36] Similarly, advances in catheter-based imaging for arthroscopic/endoscopic diagnosis of HO formation could allow a clinician to bring the excitation source and detection hardware to sites of interest in a minimally invasive manner.[37] Lastly, photoacoustic imaging, which relies on ultrasound detection of thermal expansion events associated with fluorophore excitation, reduces the susceptibility to penetration depth artifacts, and recent work showed resolution detection up to 0.1 mm in pre-clinical models.[38] Using any of these techniques, the patient would be injected with a bone-specific fluorophore, and then imaged for easier, earlier resection of the HO, bypassing the tissue penetration limitations associated with optical imaging. In summary, our findings suggest NIR contrast agents may be beneficial to the early detection of HO formation and subsequent monitoring of HO turnover, and may provide a sensitive and reliable approach to detection and monitoring of HO progression and therapy.

ACKNOWLEDGMENTS

This study was supported by NIH grant R01 AR056646, K08 GM109105, and the Plastic Surgery Foundation National Endowment Award. The authors thank Kathy Sweet and Bonnie Nolan for their assistance with animal care and in vivo microCT, John Baker for his help with histology, Shelley Almburg for assistance in confocal microscopy, and Basma Khoury for her assistance in ex vivo microCT imaging.

REFERENCES

1. Nauth A, Giles E, Potter BK, et al. 2012. Heterotopic ossification in orthopaedic trauma. J Orthop Trauma 26:684–688.
2. Vanden Bossche L, Vanderstraeten G. 2005. Heterotopic ossification: a review. J Rehabil Med 37:129–136.
3. Blokhuis TJ, Frölke JP. 2009. Is radiation superior to indomethacin to prevent heterotopic ossification in acetabular fractures? a systematic review. Clin Orthop Relat Res 467:526–530.
4. Burd TA, Lowry KJ, Anglen JO. 2001. Indomethacin compared with localized irradiation for the prevention of heterotopic ossification following surgical treatment of acetabular fractures. J Bone Joint Surg Am 83:1783–1788.
5. Cullen N, Perera J. 2009. Heterotopic Ossification: pharmacologic options. J Head Trauma Rehabil 24:69–71.
6. Moore KD, Goss K, Anglen JO. 1998. Indomethacin versus radiation therapy for prophylaxis against heterotopic ossification in acetabular fractures: a randomised, prospective study. J Bone Joint Surg Br 80:259–263.
7. Ehsan A, Huang JI, Lyons M, et al. 2012. Surgical management of posttraumatic elbow arthrofibrosis. J Trauma Acute Care Surg 72:1399–1403.
8. McAuliffe JA, Wolfson AH. 1997. Early excision of heterotopic ossification about the elbow followed by radiation therapy. J Bone Joint Surg Am 79:749–755.
9. Ledermann HP, Schweitzer ME, Morrison WB. 2002. Pelvic heterotopic ossification: MR imaging characteristics. Radiology 222:189–195.
10. Seipel R, Langner S, Platz T, et al. 2012. Neurogenic heterotopic ossification: epidemiology and morphology on conventional radiographs in an early neurological rehabilitation population. Skelet Radiol 41:61–66.
11. Wick L, Berger M, Knecht H, et al. 2005. Magnetic resonance signal alterations in the acute onset of heterotopic ossification in patients with spinal cord injury. Eur Radiol 15:1867–1875.
12. Zagarella A, Impellizzeri E, Maiolino R, et al. 2013. Pelvic heterotopic ossification: when CT comes to the aid of MR imaging. Insights Imaging 4:595–603.
13. Subhawong TK, Fishman EK, Swart JE, et al. 2010. Soft-tissue masses and masslike conditions: what does CT add to diagnosis and management? AJR Am J Roentgenol 194: 1559–1567.
14. Freed JH, Hahn H, Menter R, et al. 1982. The use of the three-phase bone scan in the early diagnosis of heterotopic ossification (HO) and in the evaluation of Didronel therapy. Paraplegia 20:208–216.
15. Muheim G, Donath A, Rossier AB. 1973. Serial scintigrams in the course of ectopic bone formation in paraplegic patients. Am J Roentgenol Radium Ther Nucl Med 118:865–869.
16. Ritt P, Vija H, Hornegger J, et al. 2011. Absolute quantification in SPECT. Eur J Nucl Med Mol Imaging 38:S69–77.
17. Cassar-Pullicino VN, McClelland M, Badwan DA, et al. 1993. Sonographic diagnosis of heterotopic bone formation in spinal injury patients. Paraplegia 31:40–50.
18. Tanaka T, Rossier AB, Hussey RW, et al. 1977. Quantitative assessment of para-osteo-arthropathy and its maturation on serial radionuclide bone images. Radiology 123:217–221.
19. Kozloff KM, Quinti L, Patntirapong S, et al. 2009. Non-invasive optical detection of cathepsin K-mediated fluorescence reveals osteoclast activity in vitro and in vivo. Bone 44: 190–198.
20. Weissleder R, Ntziachristos V. 2003. Shedding light onto live molecular targets. Nat Med 9:123–128.

21. Pogue BW, Leblond F, Krishnaswamy V, et al. 2010. Radiologic and near-infrared/optical spectroscopic imaging: where is the synergy? AJR Am J Roentgenol 195:321–332.
22. Kozloff KM, Volakis LI, Marini JC, et al. 2010. Near-infrared fluorescent probe traces bisphosphonate delivery and retention in vivo. J Bone Miner Res 25:1748–1758.
23. Kozloff KM, Weissleder R, Mahmood U. 2007. Noninvasive optical detection of bone mineral. J Bone Miner Res 22: 1208–1216.
24. Pleijhuis RG, Langhout GC, Helfrich W, et al. 2011. Near-infrared fluorescence (NIRF) imaging in breast-conserving surgery: assessing intraoperative techniques in tissue-simulating breast phantoms. Eur J Surg Oncol 37:32–39.
25. O'Brien EJO, Frank CB. Shrive NG, et al. 2012. Heterotopic mineralization (ossification or calcification) in tendinopathy or following surgical tendon trauma. Int J Exp Pathol 93: 319–331.
26. Peterson JR, Okagbare PI, De La Rosa S, et al. 2013. Early detection of burn induced heterotopic ossification using transcutaneous Raman spectroscopy. Bone 54:28–34.
27. Kovar JL, Xu X, Draney D, et al. 2011. Near-infrared-labeled tetracycline derivative is an effective marker of bone deposition in mice. Analystical Biochem 416:167–173.
28. Smith L, Bigelow EM, Jepsen KJ. 2013. Systematic evaluation of skeletal mechanical function. Curr Protoc Mouse Biol 3:39–67.
29. Villanueva AR, Kujawa M, Mathews CH, et al. 1983. Identification of the mineralization front: comparison of a modified toluidine blue stain with tetracycline fluorescence. Metab Bone Dis Relat Res 5:41–45.
30. Puzas JE, Miller MD, Rosier RN. 1989. Pathologic Bone Formation. Clin Orthop Rel Res 245:269–281.
31. Peterson JR, De La Rosa S, Sun H, et al. 2014. Burn injury enhances bone formation in heterotopic ossification model. Ann Surg 259:993–998.
32. Wilkinson JM, Stockley I, Hamer AJ, et al. 2003. Biochemical markers of bone turnover and development of heterotopic ossification after total hip arthroplasty. J Orthop Res 21: 529–534.
33. Evans KN, Forsberg JA, Potter BK, et al. 2012. Inflammatory cytokine and chemokine expression is associated with heterotopic ossification in high-energy penetrating war injuries. J Orthop Trauma 26:204–213.
34. Yokota K, Sato K, Miyazaki T, et al. 2014. Combination of tumor necrosis Factor α and interleukin-6 induces mouse osteoclast-like cells with bone resorption activity both in vitro and in vivo. Arthritis Rheumatol 66:121–129.
35. Ntziachristos V, Ripoll J, Wang LV, et al. 2005. Looking and listening to light: the evolution of whole-body photonic imaging. Nature biotechnology 23:313–320.
36. Snoeks TJ, Van Driel PB, Keereweer S, et al. 2014. Towards a successful clinical implementation of fluorescence-guided surgery. Mol Imaging Biol 16:147–151.
37. Upadhyay R, Sheth RA, Weissleder R, et al. 2007. Quantitative real-time catheter-based fluorescence molecular imaging in mice. Radiology 245:523–531.
38. Deliolanis NC, Ale A, Morscher S, et al. 2014. Deep-tissue reporter-gene imaging with fluorescence and optoacoustic tomography: a performance overview. Mol Imaging Biol [Epub ahead of print]. doi: 10.1007/s11307-014-0728-1